Cardiovascular Research (2011) **90**, 28–37
doi:10.1093/cvr/cvq378

Arterial injury promotes medial chondrogenesis in *Sm22* knockout mice

Jianbin Shen[1,2], Maozhou Yang[1,3], Hong Jiang[1], Donghong Ju[1], Jian-Pu Zheng[1], Zhonghui Xu[1,2], Tang-Dong Liao[4], and Li Li[1,2,5]*

[1]Department of Internal Medicine, Wayne State University, 421 E. Canfield Avenue, Room no. 1107, Detroit, MI 48201, USA; [2]Center for Molecular Medicine and Genetics, Wayne State University, Detroit, MI, USA; [3]Bone and Joint Center, Henry Ford Hospital, Detroit, MI, USA; [4]Department of Internal Medicine, Henry Ford Hospital, Detroit, MI, USA; and [5]Cardiovascular Research Institute, Wayne State University, Detroit, MI, USA

Received 20 April 2010; revised 8 November 2010; accepted 26 November 2010; online publish-ahead-of-print 22 December 2010

Time for primary review: 41 days

Aims Expression of SM22 (also known as SM22alpha and transgelin), a vascular smooth muscle cells (VSMCs) marker, is down-regulated in arterial diseases involving medial osteochondrogenesis. We investigated the effect of SM22 deficiency in a mouse artery injury model to determine the role of SM22 in arterial chondrogenesis.

Methods and results *Sm22* knockout (*Sm22*$^{-/-}$) mice developed prominent medial chondrogenesis 2 weeks after carotid denudation as evidenced by the enhanced expression of chondrogenic markers including type II collagen, aggrecan, osteopontin, bone morphogenetic protein 2, and SRY-box containing gene 9 (SOX9). This was concomitant with suppression of VSMC key transcription factor myocardin and of VSMC markers such as SM α-actin and myosin heavy chain. The conversion tendency from myogenesis to chondrogenesis was also observed in primary *Sm22*$^{-/-}$ VSMCs and in a VSMC line after *Sm22* knockdown: SM22 deficiency altered VSMC morphology with compromised stress fibre formation and increased actin dynamics. Meanwhile, the expression level of Sox9 mRNA was up-regulated while the mRNA levels of myocardin and VSMC markers were down-regulated, indicating a pro-chondrogenic transcriptional switch in SM22-deficient VSMCs. Furthermore, the increased expression of SOX9 was mediated by enhanced reactive oxygen species production and nuclear factor-κB pathway activation.

Conclusion These findings suggest that disruption of SM22 alters the actin cytoskeleton and promotes chondrogenic conversion of VSMCs.

Keywords Vascular smooth muscle cell • SM22 • Chondrogenesis • Reactive oxygen species • NF-κB

1. Introduction

Vascular smooth muscle cells (VSMCs) have the capacity to undergo drastic phenotypic modulation from contractile and differentiated state to proliferative, dedifferentiated, chondrocytic, and osteoblastic phenotypes in arterial diseases such as atherosclerosis and in vascular complications due to diabetes.[1–4] Arterial chondrogenesis and osteogenesis lead to increased artery stiffness and compromised blood pressure regulation capacity, thus contributing to chronic heart failure.[3,4] Medial VSMCs play essential roles in this process, as evidenced by the trans-differentiation of VSMCs to osteochondrocytic cells.[4–7] VSMC chondrogenic transdifferentiation features syntheses and deposition of distinct extracellular matrix (ECM) proteins in the arterial media, such as type II collagen, aggrecan, and osteopontin.[3–6] Expression of VSMC cytoskeleton proteins, including SM22, is down-regulated in the pathogenesis of arterial diseases and VSMCs exhibit distinct morphological changes.[4–6,8] In order to address the question of whether this down-regulation of SM22 is just a passive outcome or an active pro-chondrogenic driving force, we analysed the phenotypes of SM22 knockout mice in an artery injury model.

SM22, also known as SM22α or transgelin, is a 22 kDa protein highly expressed in smooth muscle cells (SMCs) of vertebrates during embryogenesis and in adult.[9–11] SM22 shares sequence homology with calponin and bundles actin to facilitate the formation of cytoskeletal structure such as stress fibre.[10,12] The expression of SM22 is required for modulating vessel contractility.[13] SM22 may also be involved in pathogenesis of a variety of human diseases such as cancers.[14] Interestingly, expression of *SM22* is down-regulated in osteochondrogenic atherosclerotic coronary arteries.[8] In a mouse

* Corresponding author. Tel: +1 313 577 8749; fax: +1 313 577 8615, Email: lili@med.wayne.edu

atherosclerosis model, transcription of *Sm22* decreased in atherosclerotic plaques of apolipoprotein E (ApoE)$^{-/-}$mice.[15] A body of research using both animal models and *in vitro* VSMCs corroborates down-regulation of SM22 during arterial osteochondrogenesis.[5] These data strongly suggest that disruption of SM22 may be involved in osteochondrogenesis in arterial diseases.

Nevertheless, *Sm22* knockout (*Sm22*$^{-/-}$) mice displayed uncompromised vasculature development and morphology with normal blood pressure and heart rate.[16–18] This suggests that SM22 may be functionally redundant or compensated during vasculature development.[17,18] In contrast, loss of SM22 in *ApoE*$^{-/-}$mice led to enlarged atherosclerotic lesions,[19] suggesting that loss of SM22 function might not be compensated in arterial injury. Consistent with this notion, we recently found that *Sm22*$^{-/-}$ mice showed enhanced inflammatory response upon carotid denudation.[20]

During the characterization of the role of SM22 deficiency in pro-inflammatory response, we observed prominent medial chondrogenesis after carotid injury in the same *Sm22*$^{-/-}$ mice. To explore the underlying mechanisms, we analysed the effects of SM22 disruption on medial chondrogenesis using *Sm22*$^{-/-}$ mice, primary *Sm22*$^{-/-}$VSMCs, and a rat pulmonary artery VSMC line (PAC1[21]) after *Sm22* knockdown. Here, we reported that disruption of SM22 increased actin dynamics, down-regulated smooth muscle key regulator myocardin transcripts, and up-regulated chondrogenic key regulator SRY-box containing gene 9 (*Sox9*) transcripts; this suggests that disruption of SM22 may promote VSMC transcriptional conversion from myogenesis to chondrogenesis.

2. Methods

Expanded descriptions are available in the Supplementary material online.

2.1 Animal model

The animal investigation conforms to the Guide for the Care and Use of Laboratory Animals published by the US National Institutes of Health (NIH Publication no. 85–23, revised 1996). Generation and characterization of Sm22$^{-/-}$ mice are described in our previous work.[18] The mouse carotid denudation protocol was approved by the Animal Investigation Committee at Wayne State University. Carotid denudation [22] was carried out on male *Sm22*$^{-/-}$ mice and their wild-type littermates on a mixed C57BL/6 × SV129 genetic background at 18–20 weeks of age. Briefly, after anaesthesia of mice using 2% avertin intraperitoneally (0.25 mg/g body weight), a curved guide wire of 0.35 mm in diameter was introduced into the left common carotid with constant rotation for three passages. Two weeks after surgery, the mice were sacrificed and both carotids were harvested for either embedding or RNA extraction. For embedding, the carotid segments of 3 mm in length covering the part from 2 to 5 mm proximal to the carotid bifurcation were embedded in OCT medium (Tissue-Tek), and around 100 frozen slides were made for each mouse with triplicate sections on each slide at 8 μm thickness. For RNA extraction, the carotids were stored separately in RNAlater reagent (Ambion) at 4°C for no more than 1 week before RNA extraction.

2.2 Immunohistochemistry analyses

Immunohistochemistry (IHC) was performed on consecutive frozen slides using VECTASTAIN Elite ABC Kit (Vectorlabs). Briefly, air-dried slides were fixed in methanol containing 0.3% H_2O_2 for 10 min and serum-blocked for 20 min. The following incubation steps of primary antibody, secondary antibody, ABC reagent, and DAB substrate were performed according to the manufacturer's protocol. The slides were counterstained with haematoxylin. The primary antibodies (1:50 dilution) were rabbit anti-type II collagen IgG (Abcam, ab53047), rabbit anti-aggrecan (Santa Cruz, sc-25674), goat anti-SPP1 (Santa Cruz, sc-10593), rabbit anti-bone morphogenetic protein 2 (anti-BMP2) (Abcam, ab14933), and rabbit anti-SOX9 (Abcam, ab3697). Semi-quantitative analyses were performed using the integrative optical density function in Image-Pro software.

2.3 Alcian blue staining

Alcian blue staining was performed using the Alcian blue, pH 2.5 kit (VWR International, LLC), and nuclei were counterstained with Fast Red.

2.4 Primary VSMC culture

VSMCs were isolated from mouse aorta as described.[23] Primary VSMCs were kept in the DMEM medium containing 10% foetal bovine serum and passed upon confluence at a 1:2 dilution ratio. Primary VSMCs from passage 2 to passage 4 were used for experiments.

2.5 *Sm22* knockdown in PAC1 cells with siRNA

Sm22 knockdown was achieved using Dicer-Substrate siRNA duplexes (IDT, MMC.RNAI.N011526.5.1). PAC1 cells were seeded at 30% confluence 24 h before transfection. Transfection was performed using DharmaFECT3 (Dharmacon) with siRNA duplex or scrambled RNA duplex at 100 nM, and the FBS was diluted to 2% with media 24 h after transfection for optimal cell density. In parallel experiments, the following small molecules were added 24 h after transfection: the NF-κB inhibitors Bay-11-7082 (10 μM) or IMD-0354 (200 nM), or the reactive oxygen species (ROS) scavenger Tiron (5 mM). Cells were used for experiments 72 h after transfection unless otherwise specified.

2.6 Real-time RT–PCR

Total RNA from carotids was extracted and purified using RNeasy Fibrous Tissue Kit (Qiagen), and total RNA from primary VSMCs or PAC1 cells was extracted using RNeasy Kit (Qiagen). The cDNA was synthesized using the Superscript II reverse transcriptase (Invitrogen). Real-time PCR was performed using SYBR Green on a StepOnePlus system (Applied Biosystems). GAPDH and snRNA U6 were used as internal controls in the ΔΔCt method.

2.7 Immunofluorescence analyses

PAC1 cells on chamber slides were fixed in methanol for 10 min at −20°C and blocked with 10% chicken serum for 30 min. Then, cells were incubated with primary antibodies at 1:100 dilution for 2 h followed by incubation with Alexa Fluor chicken anti-rabbit IgG (Invitrogen, A21441) and Alexa Fluor chicken anti-mouse IgG (Invitrogen, A21201) at 1:200 dilution (Invitrogen) for 1 h. Slides were mounted with Vectashield with DAPI (Vectorlabs) and examined on a Leica DM4000B microscope. Quantification was performed using Image-Pro software. Primary antibodies were rabbit anti-SM22 IgG (Abcam, ab14106) and mouse anti-smooth muscle alpha-actin (SMA) IgG2a (Santa Cruz, sc-58669).

2.8 Western blotting

Equal amount of whole-cell lysates, the nuclear fraction, or cytoplasmic fraction from primary VSMCs or PAC1 cell samples were loaded on a 4–12% Bis–Tris NuPAGE Mini-gel (Invitrogen) for electrophoresis, followed by transfer onto an Immobilon-P membrane (Millipore). The membrane was subject to chemiluminescence detection using SuperSignal West Pico Chemiluminescent Substrate (Pierce). The primary antibodies were rabbit anti-SM22 IgG (1:1000, Abcam, ab14106), rabbit anti-SMA IgG(1:500, Abcam, ab5694), rabbit anti-SOX9 (1:100, Santa Cruz, sc-20095), goat anti-Myocardin (1:100, Santa Cruz, sc-21561), and rabbit anti-GAPDH (1:2500, Abcam, ab9485).

2.9 Measurement of F/G-actin ratio

The F/G-actin ratio in PAC1 cells was determined using the G-actin/F-actin *in vivo* assay kit (Cytoskeleton Inc.) according to manufacturer's protocol. Briefly, PAC1 cells were homogenized in cell lysis and F-actin stabilization buffer containing the protease inhibitor cocktail. Centrifugation was performed for 2 h at 70 000*g* at 37°C to separate the F-actin from G-actin pool and supernatants (G-actin) were collected after centrifugation. The pellets (F-actin) were resuspended in ice-cold ddH2O containing 1 μmol/L cytochalasin D, followed by incubation and mixing on ice for 1 h to dissociate F-actin. Equal amount of the supernatant (G-actin) and the resuspended pellet (F-actin) were subjected to analysis of western blotting (WB) using the rabbit anti-actin antibody in the kit. The semi-quantification was performed using the Image-Pro software.

2.10 ROS detection

ROS in live PAC1 cells on chamber slides was detected using dihydroethidium (DHE) for superoxide (10 μM at 37°C for 10 min) and the dichlorofluorescein diacetate (DCFDA)-based Image-iT^{TM} LIVE Green ROS detection kit (Invitrogen) for peroxide (25 μM at 37°C for 30 min). Semi-quantitative analyses were performed on 30 microscopic images of each group using the integrative optical density function in Image-Pro software.

2.11 Statistics

Five $Sm22^{-/-}$ mice and five $Sm22^{+/+}$ littermates were used in IHC and real-time RT–PCR (rtRT–PCR) analyses. Primary VSMCs from four $Sm22^{-/-}$ mice and four $Sm22^{+/+}$ mice were used for rtRT–PCR analyses. Three independent experiments were performed in *Sm22* knockdown research in PAC1 cells. Values are means ± SE. Statistical analyses were performed using SPSS13.0 software. Student's *t*-test was applied to evaluate differences in all experiments and differences were considered significant at $P < 0.05$.

3. Results

3.1 Enhanced medial chondrogenesis with compromised myogenesis in $Sm22^{-/-}$ mice after carotid injury

Carotids were harvested 2 weeks after carotid denudation. IHC analysis showed remarkable expression of a chondrocyte marker, type II collagen (COL2A1), in the media of $Sm22^{-/-}$ mice (*Figure 1A* and *B*) with morphology of chondrocytic cells (Supplementary material online, *Figure S1*). Alcian blue staining revealed marked expression of mucopolysaccharides and glycosaminoglycans in the media of $Sm22^{-/-}$ mice (*Figure 1D*a and *D*b). A variety of specific ECM proteins, such as aggrecan (ACAN) and osteopontin (SPP1),[24] are required during normal chondrogenesis. IHC analysis indicated that expression of both ACAN (*Figure 2A*) and SPP1 (Supplementary material online, *Figure S2*) in the media was significantly higher in $Sm22^{-/-}$ mice compared with their $Sm22^{+/+}$ littermates. These data support a pro-chondrogenic ECM environment in injured arteries of $Sm22^{-/-}$ mice. Furthermore, BMP2, one of the major cytokines with pivotal roles in every step of chondrogenesis,[24] was intensely expressed in injured carotid media of $Sm22^{-/-}$ mice (*Figure 2B*).

In order to explore the molecular mechanisms underlying the ectopic chondrogenesis, we examined expression of Sox9, a master transcription factor regulating chondrogenesis.[24,25] IHC results showed marked SOX9 expression in the media of the injured carotids from $Sm22^{-/-}$ mice in contrast to the scant SOX9 induction from $Sm22^{+/+}$ littermates (*Figure 3A*). We also examined the mRNA level of myocardin in the media of the injured carotids. The expression of myocardin decreased significantly in injured carotids of $Sm22^{-/-}$ mice compared with that of their $Sm22^{+/+}$ littermates (60 vs. 20%, *Figure 3B*), suggesting a lower pro-myogenic tendency in the VSMCs of $Sm22^{-/-}$ mice after injury. The expression of smooth muscle myosin heavy chain (*Myh11*) was reduced, although this reduction is not statistically significant (*Figure 3B*). However, the expression of smooth muscle alpha-actin (*Acta2*) mRNA was not much affected (*Figure 3B*). This could be due to the fact that Acta2 is also expressed in adventitial cells after injury in addition to medial VSMCs as shown by IHC analysis of ACTA2 (Supplementary material online, *Figure S3*).

To search for evidence of medial osteogenesis and calcification, we performed the Alizarin Red staining. We did not find calcium deposition in carotids from either $Sm22^{-/-}$ mice or those from their $Sm22^{+/+}$ littermates based on the negative results of Alizarin Red staining (data not shown). Meanwhile, we analysed expression of osteocalcin (BGLAP), alkaline phosphatase, and RUNX2 using IHC and found little difference between these two groups. These results indicated lack of medial calcification at this time point.

These *in vivo* findings illustrate a transcriptional shift from pro-myogenesis to pro-chondrogenesis in the arteries of $Sm22^{-/-}$ mice upon stress; this suggests that loss of SM22 in VSMCs might promote the ectopic medial chondrogenesis via transcriptional switch.

3.2 A transcriptional shift from myogenic to chondrogenic pattern in primary $Sm22^{-/-}$ VSMCs and after *Sm22* knockdown in a VSMC line

To explore the transcriptional changes after SM22 disruption in VSMCs, we investigated expression of several marker genes in primary VSMCs from $Sm22^{-/-}$ mice and their $Sm22^{+/+}$ littermates and in PAC1 cells after *Sm22* knockdown. The mRNA levels of *Myocd, Smtn, Acta2,* and *Myh11* in $Sm22^{-/-}$ VSMCs were lower than those in $Sm22^{+/+}$ VSMCs (*Figure 4A*), while the mRNA levels of *Sox9*, *Bmp2* and *Col2a1* were higher in $Sm22^{-/-}$ VSMCs (Figure 4A). The expressions of ACTA2 and SOX9 proteins were also decreased and increased, respectively, in $Sm22^{-/-}$ VSMCs by WB (*Figure 4A*, the insert panel). We failed to detect the MYOCD protein in primary VSMCs by WB. In PAC1 cells, the decrease of *Myocd*, *Smtn*, *Acta2*, and *Myh11* mRNA correlated with the increased *Sm22* knockdown efficiency over time after siRNA treatment (*Figure 4B*). In contrast, the expression of *Sox9* mRNA gradually increased (*Figure 4B*), although the mRNA levels of *Col2a1* and *Acan* were not up-regulated in the VSMC culture conditions (data not shown). Accordingly, WB revealed decreased expression of MYOCD and ACTA2 and increased expression of SOX9 in PAC1 3 days after *Sm22* siRNA treatment (*Figure 4B*, insert panel). In contrast, knockdown of *Acta2* or *Myh11* in PAC1 cells did not increase expression of Sox9 (data now shown). These data suggest a switch from myogenesis to chondrogenesis in VSMCs after SM22 disruption: this led us to ask how disruption of an actin cytoskeletal protein alters VSMC fate.

3.3 Compromised phenotype in primary $Sm22^{-/-}$ VSMCs and in PAC1 cells after *Sm22* knockdown

Disruption of actin cytoskeleton and increased actin dynamics in mesenchymal cells are known to lead to chondrogenesis.[26] Since

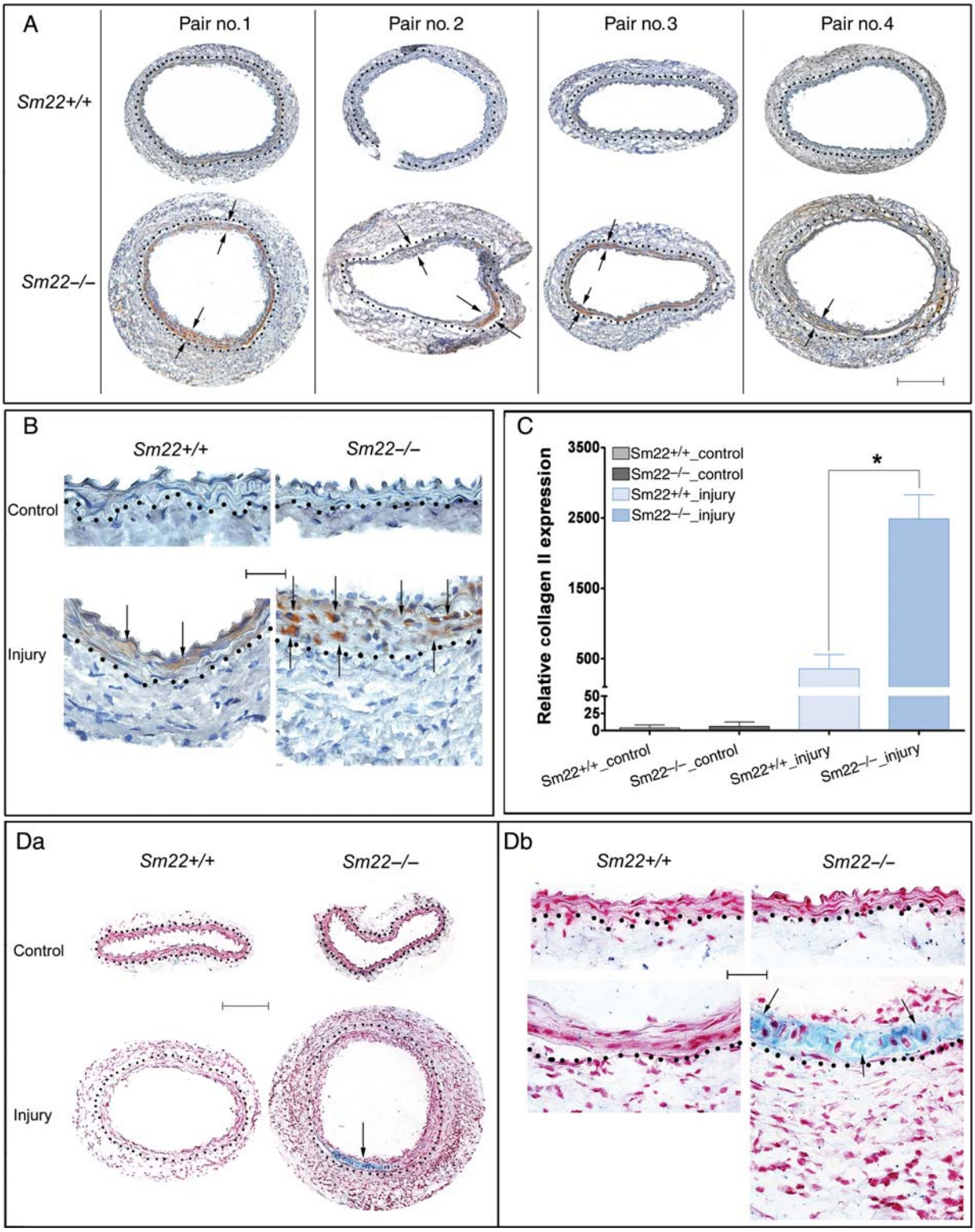

Figure 1 Enhanced type II collagen in $Sm22^{-/-}$ mice 2 weeks after carotid denudation. Expression of type II collagen was evaluated by IHC. (*A*) Injured carotids from four $Sm22^{-/-}$ mice and their wild-type littermates at 100× magnification are shown. (*B*) Both injured carotids and non-injured controls at 400× magnification. Representative brown signals were indicated by the arrows. (*C*) Quantification of positive signals from images at 100× magnification in the media of carotids from five $Sm22^{-/-}$ and their littermates $Sm22^{+/+}$ mice. (*D*) Alcian blue staining of carotids at 100× (Da) and at 400× magnification (*Db*). Blue signals, Alcian blue; red signals, nuclear fast red. Bar in (*A* and *Da*), 100 μm; bar in (*B* and *Db*), 20 μm. Dashed lines demarcated the border between media and adventitia. Values are means ± SE. The asterisk indicates $P < 0.05$ vs. $Sm22^{+/+}$ mice.

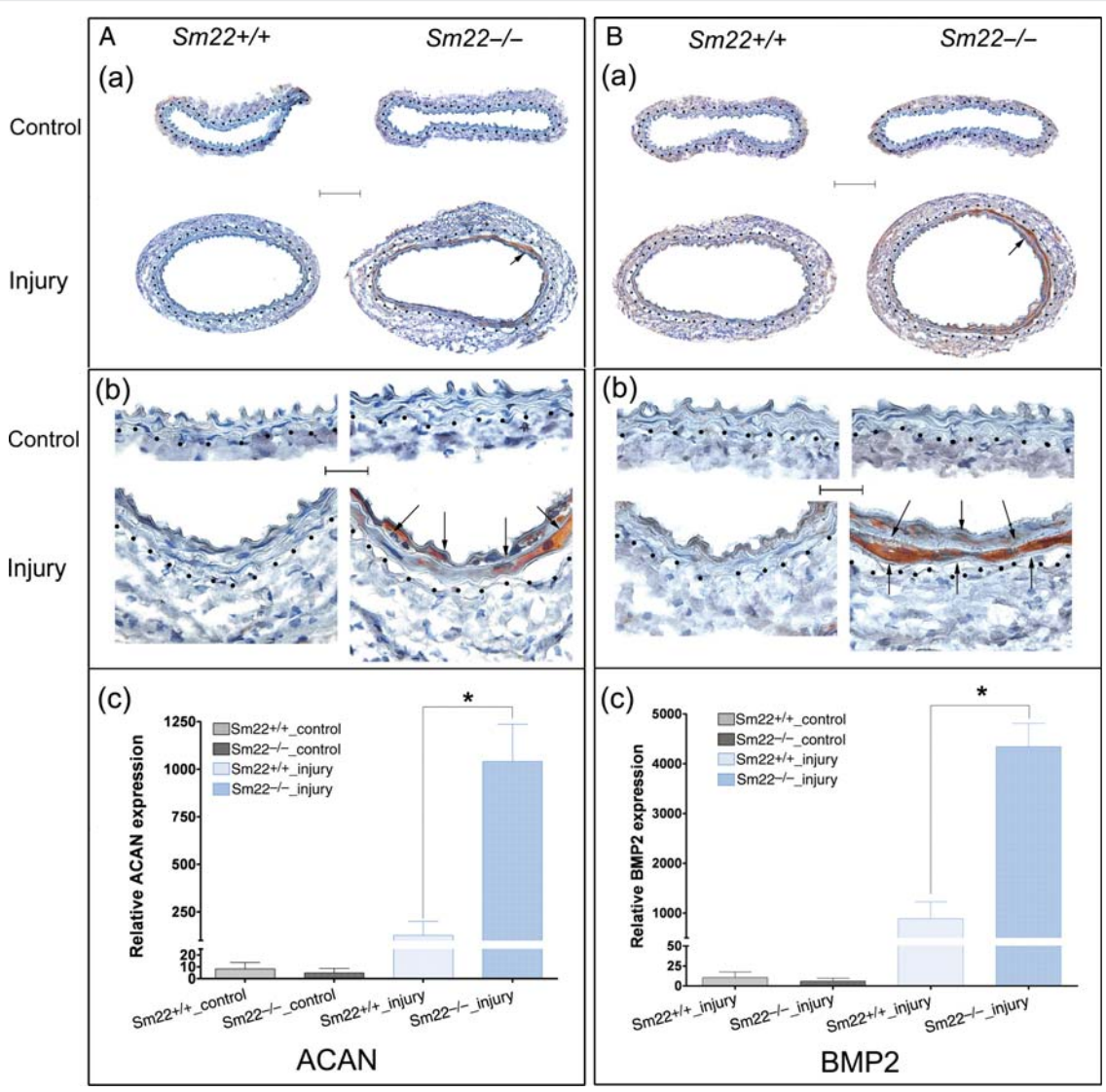

Figure 2 Augmented expression of aggrecan and BMP2 in $Sm22^{-/-}$ mice 2 weeks after carotid denudation. (*A*) IHC analyses of ACAN (a) at 100× magnification, (b) at 400× magnification and (c) quantification of positive signals from images at 100× magnification in the media of carotids from five $Sm22^{-/-}$ and their littermates $Sm22^{+/+}$ mice. (*B*) IHC analyses of BMP2 (a) at 100× magnification, (b) at 400× magnification and (c) quantification of positive signals from images at 100× magnification in the media of carotids from five $Sm22^{-/-}$ and their littermates $Sm22^{+/+}$ mice. Representative brown signals are indicated by the arrows. Bars in (*Aa*) and (*Ba*), 100 μm; bars in (*Ab*) and (*Bb*), 20 μm. Dashed lines demarcated the border between media and adventitia. Values in (*Ac*) and (*Bc*) are means ± SE. The asterisks indicate $P < 0.05$ vs. $Sm22^{+/+}$ mice.

SM22 is an actin-binding protein, we propose that disruption of SM22 might affect actin cytoskeleton and actin dynamic. After passage 2, the primary $Sm22^{-/-}$ VSMCs displayed remarkable morphological changes, in which they lost their spindle-shaped appearance and became spherical (*Figure 5A*). We observed similar morphological change after *Sm22* knockdown in PAC1 cells (*Figure 5B*). We then used immunofluorescence (IF) to visualize the actin cytoskeleton in PAC1 cells. Abundant actin stress fibres co-localized with SM22 in control PAC1 cells (*Figure 5C* and Supplementary material online, *Figure S4*, upper panel). However, there was scant actin stress fibre formation after *Sm22* knockdown (*Figure 5C* and Supplementary material online, *Figure S4*, lower panel). We further evaluated actin dynamics by the G/F-actin ratio and found a significant increase (ca. three-fold) of the G/F-actin ratio after *Sm22* knockdown (*Figure 5D*). These alterations in cell morphology and actin dynamics could be indications of chondrogenic shift of VSMCs.

3.4 Boosted ROS production after *Sm22* knockdown in PAC1 cells contributed to *Sox9* induction

Expression of *Sox9* can be activated by ROS-dependent transcription factors during developmental chondrogenesis.[27] Thus, we hypothesized that the up-regulation of *Sox9* might be initiated by ROS increase after *Sm22* knockdown in PAC1 cells. Indeed, we recently showed that disruption of SM22 expression by *Sm22* knockdown in PAC1 cells boosted ROS production as measured by the superoxide marker DHE and the peroxide marker DCFDA-based assays.[20] For

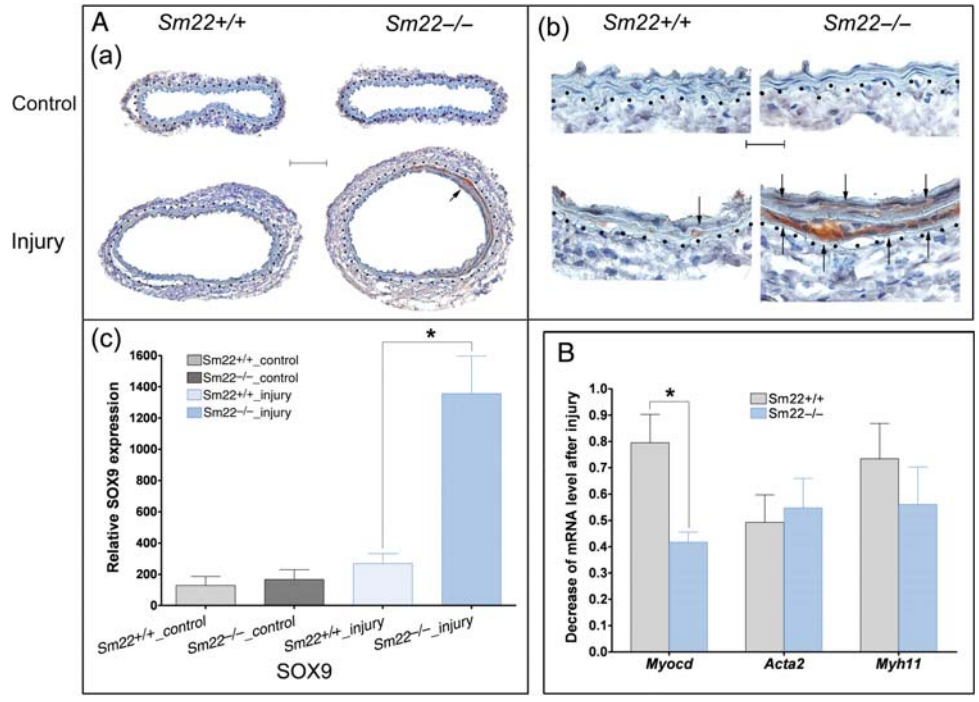

Figure 3 Up-regulation of Sox9 expression and down-regulation of Myocd expression in $Sm22^{-/-}$ mice 2 weeks after carotid denudation. (*A*) IHC analyses of SOX9 (a) at 100× magnification, (b) at 400× magnification and (c) quantification of positive signals from images at 100× magnification in the media of carotids from five $Sm22^{-/-}$ and their littermates $Sm22^{+/+}$ mice. Representative brown signals were indicated by the arrows. Bar in (*Aa*), 100 μm; bar in (*Ab*), 20 μm. (*B*) Relative mRNA level of Myocd, Acta2 and Myh11 in injured carotids was evaluated using rtRT–PCR. Dashed lines demarcated the border between media and adventitia. Values in (*Ac*) and (*B*) are means ± SE. The asterisks indicate $P < 0.05$ vs. $Sm22^{+/+}$ mice.

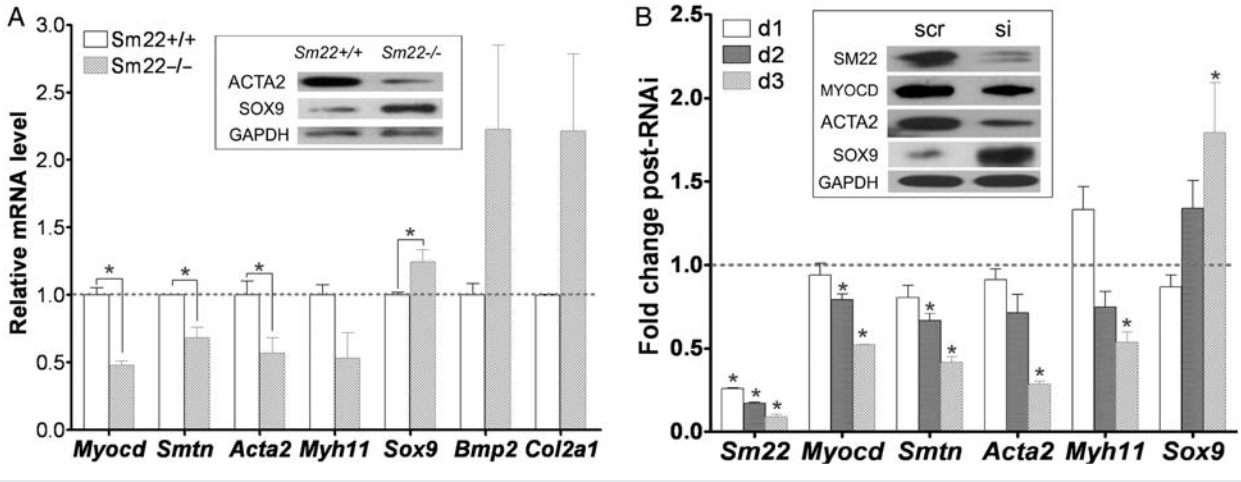

Figure 4 Chondrogenic switch of VSMCs in primary $Sm22^{-/-}$ VSMCs and in PAC1 cells after Sm22 knockdown. (*A*) In primary $Sm22^{-/-}$ and $Sm22^{+/+}$ VSMCs, relative mRNA expression of Myocd, Smtn, Acta2, Myh11, Sox9, Bmp2 and Col2a1 was examined using rtRT–PCR and WB (insert panel). Values are means ± SE from primary VSMCs of four pairs of mice. The asterisks indicate $P < 0.05$ vs. $Sm22^{+/+}$ VSMCs. (*B*) In PAC1 cells, Sm22 knockdown efficiency and the expression of Myocd, Smtn, Acta2, Myh11 and Sox9 were determined by rtRT–PCR 1 day, 2 days and 3 days after transfection, and by WB (insert panel) 3 days after transfection. Values are means ± SE from three independent experiments. The asterisks indicate $P < 0.05$ vs. the scr group. Abbreviations: scr, scrambled siRNA; si, Sm22 siRNA; d1/2/3, 1/2/3 days after transfection into PAC1 cells.

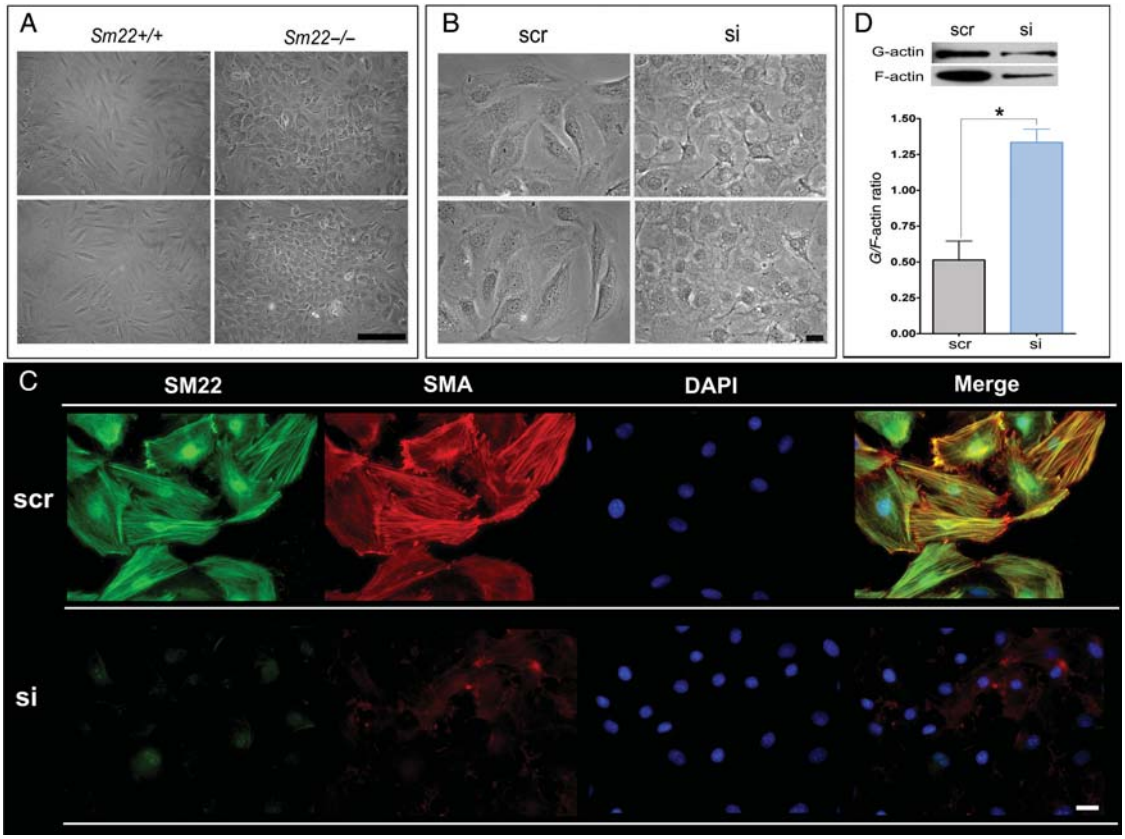

Figure 5 Compromised phenotype in primary Sm22$^{-/-}$ VSMCs and in PAC1 cells after Sm22 knockdown. (*A*) Two views of phase-contrast images from primary Sm22$^{-/-}$ and Sm22$^{+/+}$ VSMCs at passage 4. Bar, 50 μm. (*B*) The phase-contrast images from PAC1 cells in the absence or presence of Sm22 siRNA. Bar, 20 μm. (*C*) Expression of SM22 and SMA was investigated using IF. Bars, 20 μm. (*D*) Actin dynamics was determined by G/F-actin ratio in PAC1 cells without or with Sm22 siRNA. Values are means ± SE from three independent experiments. The asterisks indicate $P < 0.05$ vs. the scr group.

easy comparison, we show this boosted ROS production after *Sm22* knockdown (*Figure 6A*, si group vs. scr group). To inspect whether the elevated ROS contributes to *Sox9* induction after *Sm22* knockdown, we abolished ROS increase using an ROS scavenger, Tiron (*Figure 6A*, si + Ti group vs. si group). After interference by Tiron upon *Sm22* knockdown, transcriptional activation of *Sox9* was significantly suppressed (*Figure 6A*, *Sox9* columns, si + Ti group vs. si group). Accordingly, increased expression of the SOX9 protein was also suppressed by Tiron as shown by WB analyses (*Figure 6A*, insert panel). These investigations suggest that *Sm22* knockdown augmented ROS production, thus activating ROS-sensitive transcriptional machinery and promoting *Sox9* expression. This leads to the question of how increased ROS production leads to transcriptional activation of *Sox9*.

3.5 The redox-sensitive NF-κB signalling pathway was involved in *Sox9* induction

As a typical redox-sensitive signalling pathway, the NF-κB signalling pathway was recently shown to participate in *Sox9* expression and chondrogenesis.[28,29] We reported that the NF-κB pathway is activated after *Sm22* knockdown in PAC1 cells and is associated with boosted ROS production.[20] Thus, we tested whether NF-κB activation contributed to the up-regulation of *Sox9* after *Sm22* knockdown. After inhibition of the NF-κB pathway during *Sm22* knockdown in PAC1 cells using NF-κB inhibitors, Bay-11−7082 or IMD-0354, transcriptional activation of *Sox9* was significantly reduced (*Figure 6B*). Consistently, WB results showed that increased SOX9 protein was suppressed by Bay-11−7082 (*Figure 6B*, insert panel). These results suggest that NF-κB pathway activation mediates the transcriptional activation of *Sox9* after *Sm22* knockdown.

4. Discussion

The results presented above show that SM22 deficiency in VSMCs promoted conversion of medial VSMCs into chondrogenic cells in response to artery injury. This notion is further supported by *in vitro* experiments using primary VSMCs from *SM22*$^{-/-}$ mice and PAC1 after *SM22* knockdown. The underlying molecular mechanisms are proposed in *Figure 6C*: disruption of SM22 expression in VSMCs may hamper cytoskeleton formation and inhibit VSMC differentiation in part by suppressing myocardin expression; it may also promote chondrogenic differentiation by inducing expression of Sox9 via a signalling pathway involving ROS and NF-κB.

4.1 Arterial chondrogenesis and limitations of current *in vivo* model

Although arterial chondrogenesis occurs in the diseased vessel wall, it may share certain common cellular and molecular events and signalling pathways with chondrogenesis during normal development.[3,4,24]

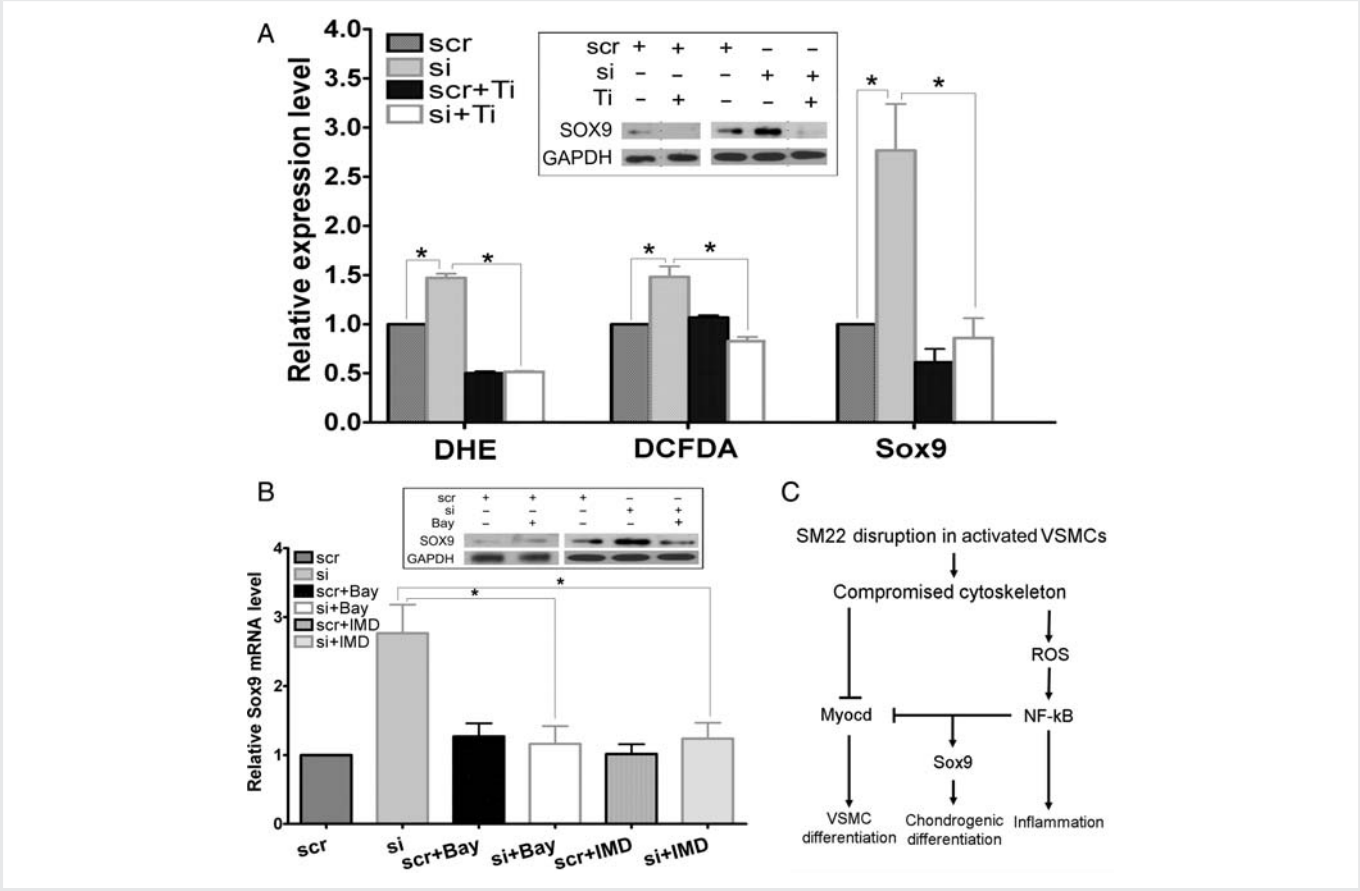

Figure 6 Elevated ROS production and NF-κB activation contributed to up-regulation of Sox9 after Sm22 knockdown in PAC1 cells. (*A*) ROS levels in PAC1 in the absence or presence of Sm22 siRNA cells were evaluated using DHE- and DCFDA-based fluorescence microscopy, and an ROS scavenger, Tiron, was applied. Thirty images were taken, respectively, each group. Sox9 expression was investigated using rtRT–PCR (Sox9 bars) and WB (insert panel) in PAC1 cells treated with Sm22 siRNA in the presence or absence of Tiron as indicated. (*B*) Suppression of Sox9 induction after Sm22 knockdown using two NF-κB pathway inhibitors, Bay-11–7082 (Bay) or IMD-0354 (IMD) was evaluated using rtRT–PCR and WB (insert panel). Values in (*A*) and (*B*) are means ± SE from three independent experiments. The asterisks indicate $P < 0.05$ between two compared groups. (*C*) Schematic representation of the transcriptional shift from myogenesis to chondrogenesis upon SM22 disruption in VSMCs.

First, a variety of ECM proteins are expressed distinctly in different stages of chondrogenesis. Proliferation and differentiation of chondroprogenitors are maintained by the ECM structure composed of type II collagen, a hallmark of chondrogenesis, and aggrecan, a major chondrogenic proteoglycan.[24] Chondrocyte terminal differentiation hypotrophy and calcification correlate with the expression of such ECM proteins as osteopontin and osteocalcin.[5,6,24] In the media of injured carotids of $Sm22^{-/-}$ mice, we observed high expression of ECM proteins, including type II collagen, aggrecan, osteopontin, and type I collagen a2, a fibrosis marker (data not shown). This suggests the existence of a pro-chondrogenic ECM environment in the injured carotids of $Sm22^{-/-}$ mice. However, injury-induced up-regulation of matrix GLA protein (MGP), a key anti-chondrogenic ECM protein,[5] was similar between $Sm22^{-/-}$ and $Sm2^{-+/+-}$ mice (Supplementary material online, *Figure S5*), suggesting that the regulation of chondrogenesis is context dependent. Second, BMP2 is a cytokine with multifaceted functions required for almost every stage of chondrogenesis[24]: we did find that *Bmp2* is highly induced in the media of injured carotids of $Sm22^{-/-}$ mice. Finally, the key transcriptional regulator of chondrogenesis, SOX9, is also highly expressed,[24,25] reflecting the activation of pro-chondrogenic transcription in the media of the injured $Sm22^{-/-}$ carotid.

Our *in vivo* results suggest that down-regulation of SM22 may expedite arterial chondrogenesis. This may, at least in part, explain why down-regulation of VSMC markers including SM22 is found in arterial calcification with prominent osteochondrogenic cells.[4–6,8] Nevertheless, it is still unclear whether this pro-chondrogenic property of the injured arteries in $Sm22^{-/-}$ mice derives from the VSMCs or from other types of cells in the artery wall since the conventional IF assay gave high background due to the injury-induced inflammation. Besides, we only observed marginal neointima formation in injured carotids: this might be due to the C57Bl/6-based mixed genetic background that may be resistant to injury-induced neointima formation.[30] It is also noteworthy that we did not gain evidence of arterial calcification. There are at least two possibilities: either that the terminal stage of endochondral calcification requires an extended process beyond the 2-week period in the current injury model, or that arterial chondrogenesis could exist as an independent state free of calcification. To answer this question, prolonged post-injury time in the carotid denudation model or other injury models could be used in further study.

4.2 Chondrogenic phenotypic modulation of VSMCs and limitations of the *in vitro* model

VSMCs are highly plastic and undergo multifaceted phenotypic changes during the pathogenesis of arterial diseases. Under physiological condition, VSMCs express an array of VSMC contractile and cytoskeleton proteins. In response to injury, VSMCs lose their contractile phenotype, increase actin dynamics, and acquire the phenotypes of other cell types including chondrocytic cells.[2,5,7,31] The cell fate is determined by the interplay of key transcriptional factors and signal pathways, which down-regulates VSMC markers and up-regulates markers of other lineages.

It is known that VSMCs derive from mesenchymal cells and that disruption of actin cytoskeleton with increased actin dynamics in mesenchymal cells leads to chondrogenesis.[26] Therefore, disrupted actin stress fibres and loss of VSMC morphology may be indicative of chondrogenic conversion. We observed similar morphological alteration from the spindle-shaped appearance typical of differentiated VSMCs to the spherical appearance of chondrocytes in primary *Sm22*$^{-/-}$ VSMCs and PAC1 cells after *Sm22* knockdown. Furthermore, knockdown of *Sm22* resulted in compromised actin stress fibre formation and increased actin dynamics: this agrees with the findings in a VSMC primary culture system treated with antisense *Sm22*.[32]

Cell structural changes are often associated with transcriptional reprogramming, and morphological changes in early endochondral bone formation correlate with the activation of chondrogenic transcription.[24,27] Among others, SOX9 is one key transcription factor that controls the expression of chondrogenic ECM proteins, including type II collagen and aggrecan.[24,25] On the other hand, myocardin is a master transcription factor of VSMCs since it is necessary and sufficient to transactivate SMC markers, including SMA and SM22.[33,34] In our *in vitro* investigation, along with the cell morphological transformation after *Sm22* knockdown, the suppressed myocardin expression and augmented expression of *Sox9* were consistent with such a transcriptional shift favouring chondrogenesis over myogenesis. Intriguingly, we also found that *Sox9* induction after *Sm22* knockdown is mediated via ROS-sensitive NF-κB pathway activation, which agrees with the known mechanism of *Sox9* activation.[28,29] However, it is unlikely that this ROS–NF-κB pathway mediates down-regulation of myocardin since both ROS inhibitors and NF-κB inhibitors failed to prevent its down-regulation (data not shown). Alternative mechanisms including microRNAs may be tested in further experiments. It is worth noting that oxidative stress promotes VSMC osteogenic conversion by inducing the expression of Runx2, the key regulator for osteogenic differentiation.[35]

4.3 Arterial inflammation and arterial chondrogenesis: coupled or sequential?

Our recent study showed prominent inflammation in injured carotids from *Sm22*$^{-/-}$ mice;[20] the present results revealed enhanced medial chondrogenesis in the same mice. Accumulating evidence suggests that inflammation contributes to arterial osteochondrogenesis in a variety of arterial diseases.[36] It is thus reasonable to argue that the enhanced chondrogenesis is caused by the exogenous cytokines from the infiltrated inflammatory cells such as macrophages.

However, we cannot exclude the possibility that loss of SM22 autonomously couples chondrogenic conversion of VSMCs with inflammatory responses. This notion is supported by the following evidence. In SM22-disrupted VSMCs, we observed the simultaneous activation of pro-inflammatory NF-κB, induction of *Sox9* and repression of *myocd*. Since NF-κB can induce *Sox9* expression[29] (*Figure 6C*) and repress myocardin myogenic activity,[37] NF-κB may be pivotal in coupling chondrogenesis with inflammation in arterial diseases where SM22 is down-regulated. Thus, it is noteworthy that this coupling of chondrogenesis and inflammation could be independent of inflammatory cells. Therefore, disruption of SM22 in VSMCs might contribute to arterial osteochondrogenesis through at least two avenues, either directly by activating chondrogenic differentiation or indirectly by inducing pro-osteochondrogenic events as a result of VSMC inflammation.

In summary, our results show that SM22 disruption may induce the pro-inflammatory and pro-chondrogenic tendency in VSMCs. These studies may offer a glimpse on the importance of actin cytoskeleton integrity in preserving the VSMC phenotype and in maintaining artery homeostasis. Therefore, maintaining VSMC cytoskeleton gene expression in VSMCs may serve as a therapeutic strategy to treat arterial diseases.

Supplementary material

Supplementary material is available at *Cardiovascular Research* online.

Acknowledgements

The authors thank J.-P. Jin, S. Helena Kuivaniemi, Hui J. Li, Jeffrey A. Loeb and Da-zhi Wang for valuable discussion and critics.

Conflict of interest: none declared.

Funding

The National Institutes of Health (HL058916, and HL087014 to L.L.), the American Heart Association (0555680Z to L.L.) and intramural grants from Wayne State University (to L.L.).

References

1. Abedin M, Tintut Y, Demer LL. Vascular calcification: mechanisms and clinical ramifications. *Arterioscler Thromb Vasc Biol* 2004;**24**:1161–1170.
2. Iyemere VP, Proudfoot D, Weissberg PL, Shanahan CM. Vascular smooth muscle cell phenotypic plasticity and the regulation of vascular calcification. *J Intern Med* 2006; **260**:192–210.
3. Johnson RC, Leopold JA, Loscalzo J. Vascular calcification: pathobiological mechanisms and clinical implications. *Circ Res* 2006;**99**:1044–1059.
4. Demer LL, Tintut Y. Vascular calcification: pathobiology of a multifaceted disease. *Circulation* 2008;**117**:2938–2948.
5. Speer MY, Yang HY, Brabb T, Leaf E, Look A, Lin WL *et al*. Smooth muscle cells give rise to osteochondrogenic precursors and chondrocytes in calcifying arteries. *Circ Res* 2009;**104**:733–741.
6. Speer MY, McKee MD, Guldberg RE, Liaw L, Yang HY, Tung E *et al*. Inactivation of the osteopontin gene enhances vascular calcification of matrix Gla protein-deficient mice: evidence for osteopontin as an inducible inhibitor of vascular calcification *in vivo*. *J Exp Med* 2002;**196**:1047–1055.
7. Bobryshev YV. Transdifferentiation of smooth muscle cells into chondrocytes in atherosclerotic arteries *in situ*: implications for diffuse intimal calcification. *J Pathol* 2005;**205**:641–650.
8. Shanahan CM, Cary NR, Metcalfe JC, Weissberg PL. High expression of genes for calcification-regulating proteins in human atherosclerotic plaques. *J Clin Invest* 1994; **93**:2393–2402.
9. Lees-Miller JP, Heeley DH, Smillie LB. An abundant and novel protein of 22 kDa (SM22) is widely distributed in smooth muscles. Purification from bovine aorta. *Biochem J* 1987;**244**:705–709.
10. Shapland C, Hsuan JJ, Totty NF, Lawson D. Purification and properties of transgelin: a transformation and shape change sensitive actin-gelling protein. *J Cell Biol* 1993;**121**: 1065–1073.

11. Li L, Miano JM, Cserjesi P, Olson EN. SM22 alpha, a marker of adult smooth muscle, is expressed in multiple myogenic lineages during embryogenesis. *Circ Res* 1996;**78**: 188–195.
12. Fu Y, Liu HW, Forsythe SM, Kogut P, McConville JF, Halayko AJ *et al*. Mutagenesis analysis of human SM22: characterization of actin binding. *J Appl Physiol* 2000;**89**: 1985–1990.
13. Zeidan A, Sward K, Nordstrom I, Ekblad E, Zhang JC, Parmacek MS *et al*. Ablation of SM22alpha decreases contractility and actin contents of mouse vascular smooth muscle. *FEBS Lett* 2004;**562**:141–146.
14. Assinder SJ, Stanton JA, Prasad PD. Transgelin: an actin-binding protein and tumour suppressor. *Int J Biochem Cell Biol* 2009;**41**:482–486.
15. Wamhoff BR, Hoofnagle MH, Burns A, Sinha S, McDonald OG, Owens GK. A G/C element mediates repression of the SM22alpha promoter within phenotypically modulated smooth muscle cells in experimental atherosclerosis. *Circ Res* 2004;**95**: 981–988.
16. Kuhbandner S, Brummer S, Metzger D, Chambon P, Hofmann F, Feil R. Temporally controlled somatic mutagenesis in smooth muscle. *Genesis* 2000;**28**:15–22.
17. Zhang JC, Kim S, Helmke BP, Yu WW, Du KL, Lu MM *et al*. Analysis of SM22alpha-deficient mice reveals unanticipated insights into smooth muscle cell differentiation and function. *Mol Cell Biol* 2001;**21**:1336–1344.
18. Yang M, Jiang H, Li L. Sm22α transcription occurs at the early onset of the cardiovascular system and the intron 1 is dispensable for its transcription in smooth muscle cells during mouse development. *Int J Physiol Pathophysiol Pharmacol* 2010;**2**:12–16.
19. Feil S, Hofmann F, Feil R. SM22alpha modulates vascular smooth muscle cell phenotype during atherogenesis. *Circ Res* 2004;**94**:863–865.
20. Shen J, Yang M, Ju D, Jiang H, Zheng JP, Xu Z *et al*. Disruption of SM22 promotes inflammation after artery injury via nuclear factor kappaB activation. *Circ Res* 2010; **106**:1351–1362.
21. Rothman A, Kulik TJ, Taubman MB, Berk BC, Smith CW, Nadal-Ginard B. Development and characterization of a cloned rat pulmonary arterial smooth muscle cell line that maintains differentiated properties through multiple subcultures. *Circulation* 1992; **86**:1977–1986.
22. Lindner V, Fingerle J, Reidy MA. Mouse model of arterial injury. *Circ Res* 1993;**73**: 792–796.
23. Ray JL, Leach R, Herbert JM, Benson M. Isolation of vascular smooth muscle cells from a single murine aorta. *Methods Cell Sci* 2001;**23**:185–188.
24. Goldring MB, Tsuchimochi K, Ijiri K. The control of chondrogenesis. *J Cell Biochem* 2006;**97**:33–44.
25. Akiyama H, Chaboissier MC, Martin JF, Schedl A, de Crombrugghe B. The transcription factor Sox9 has essential roles in successive steps of the chondrocyte differentiation pathway and is required for expression of Sox5 and Sox6. *Genes Dev* 2002; **16**:2813–2828.
26. Lim YB, Kang SS, An WG, Lee YS, Chun JS, Sonn JK. Chondrogenesis induced by actin cytoskeleton disruption is regulated via protein kinase C-dependent p38 mitogen-activated protein kinase signaling. *J Cell Biochem* 2003;**88**:713–718.
27. Amarilio R, Viukov SV, Sharir A, Eshkar-Oren I, Johnson RS, Zelzer E. HIF1alpha regulation of Sox9 is necessary to maintain differentiation of hypoxic prechondrogenic cells during early skeletogenesis. *Development* 2007;**134**:3917–3928.
28. Yates KE. Identification of cis and trans-acting transcriptional regulators in chondroinduced fibroblasts from the pre-phenotypic gene expression profile. *Gene* 2006;**377**: 77–87.
29. Ushita M, Saito T, Ikeda T, Yano F, Higashikawa A, Ogata N *et al*. Transcriptional induction of SOX9 by NF-kappaB family member RelA in chondrogenic cells. *Osteoarthritis Cartilage* 2009;**17**:1065–1075.
30. Sindermann JR, Kobbert C, Skaletz-Rorowski A, Breithardt G, Plenz G, March KL. Vascular injury response in mice is dependent on genetic background. *Am J Physiol Heart Circ Physiol* 2006;**290**:H1307–1310.
31. Zheng JP, Ju D, Shen J, Yang M, Li L. Disruption of actin cytoskeleton mediates loss of tensile stress induced early phenotypic modulation of vascular smooth muscle cells in organ culture. *Exp Mol Pathol* 2010;**88**:52–57.
32. Han M, Dong LH, Zheng B, Shi JH, Wen JK, Cheng Y. Smooth muscle 22 alpha maintains the differentiated phenotype of vascular smooth muscle cells by inducing filamentous actin bundling. *Life Sci* 2009;**84**:394–401.
33. Wang D, Chang PS, Wang Z, Sutherland L, Richardson JA, Small E *et al*. Activation of cardiac gene expression by myocardin, a transcriptional cofactor for serum response factor. *Cell* 2001;**105**:851–862.
34. Chen J, Kitchen CM, Streb JW, Miano JM. Myocardin: a component of a molecular switch for smooth muscle differentiation. *J Mol Cell Cardiol* 2002;**34**:1345–1356.
35. Byon CH, Javed A, Dai Q, Kappes JC, Clemens TL, Darley-Usmar VM *et al*. Oxidative stress induces vascular calcification through modulation of the osteogenic transcription factor Runx2 by AKT signaling. *J Biol Chem* 2008;**283**:15319–15327.
36. Shao JS, Cheng SL, Sadhu J, Towler DA. Inflammation and the osteogenic regulation of vascular calcification: a review and perspective. *Hypertension* 2010;**55**:579–592.
37. Tang RH, Zheng XL, Callis TE, Stansfield WE, He J, Baldwin AS *et al*. Myocardin inhibits cellular proliferation by inhibiting NF-{kappa}B(p65)-dependent cell cycle progression. *Proc Natl Acad Sci USA* 2008;**105**:3362–3367.